

Acknowledgment. This research was supported in part by NIH Grant R15-GM42066.

Registry No. CoL, 60193-64-8.

Contribution from the Isotope and Structural Chemistry Group (INC-4, Mail Stop C345) and Photochemistry and Photophysics Group (CLS-4, Mail Stop J567), Los Alamos National Laboratory, Los Alamos, New Mexico 87545

Time-Resolved Infrared Spectroscopy of $\text{Rh}_2(1,3\text{-diisocyanopropane})_4(\text{BPh}_4)_2$

Stephen K. Doorn,[†] Keith C. Gordon,[†] R. Brian Dyer,^{*,†} and William H. Woodruff^{*,†}

Received December 4, 1991

Binuclear d^8 complexes have been extensively studied because of their interesting bonding characteristics, spectroscopic properties, and photochemical reactions.¹ The changes in metal-metal and metal-ligand bonding upon photoexcitation are of interest in these systems. Characterization of the excited-state bond length changes may provide an understanding of the role played by the ligands in controlling the dynamics of the excited state.

In this report, we focus on the ligand-bridged complex $\text{Rh}_2\text{b}_4^{2+}$ ($\text{b} = 1,3\text{-diisocyanopropane}$). In particular, we are interested in how the Rh-Rh, Rh-C, and C≡N bonds are displaced upon photoexcitation. From a knowledge of both the ground- and excited-state vibrational frequencies associated with these bonds, their excited-state displacements may be calculated (*vide infra*). The Rh-Rh and Rh-C frequencies are known from resonance Raman studies.² However, no reliable value for the excited-state C≡N frequency is known. We now report the time-resolved IR (TRIR) spectrum of the excited state in the 2130-2200- cm^{-1} (C≡N stretching) region.

Samples were photolyzed with 750 $\mu\text{J}/\text{pulse}$ at 532 nm (with a frequency-doubled, Q-switched Nd:YAG laser operating at 10 Hz). An infrared diode laser provided probe light, which was detected by a small-element InSb detector. Calibration of the probe wavelength was accomplished by observing the spectral output of the laser in an FTIR instrument. Signals were amplified 2500 times prior to digitization with a Tektronix Model 7912 HB transient digitizer. Digitized signals were averaged and analyzed on a Mac II computer system. Each point in the transient spectrum is calculated from the maximum deflection of the transient signal. Each transient is the average of 640-1920 laser shots. Figure 1 shows an example of the high-quality transient IR data obtained, in this case at 2173 cm^{-1} . Observed lifetimes for both the bleach and transient absorbance were 6 (± 1) μs , in agreement with that found previously for the $\text{Rh}_2\text{b}_4^{2+}$ triplet excited state.⁴ The relatively large uncertainty observed for the lifetime (± 1 μs) is attributed to variable oxygen concentration in the sample cell and not to noise in the transients.

Shown in Figure 2 is the TRIR transient difference spectrum obtained for $\text{Rh}_2\text{b}_4^{2+}$.³ This spectrum is obtained point-by-point at various IR frequencies from data such as those shown in Figure 1. The spectrum shows a bleach of the ground-state absorbance at 2193 cm^{-1} and a growth in absorbance that peaks near 2177 cm^{-1} . (The peak of the excited-state absorption band is taken as the calculated peak from the double Lorentzian fit to the data. As can be seen in Figure 2, the fit to the data is quite good and also reproduces the ground-state peak at 2193 cm^{-1} .)

Transient UV/vis absorption spectroscopy has shown that the $\text{Rh}_2\text{b}_4^{2+}$ excited state has appreciable absorbance at 532 nm,⁴ and thus excitation with intense pulses at 532 nm might result in

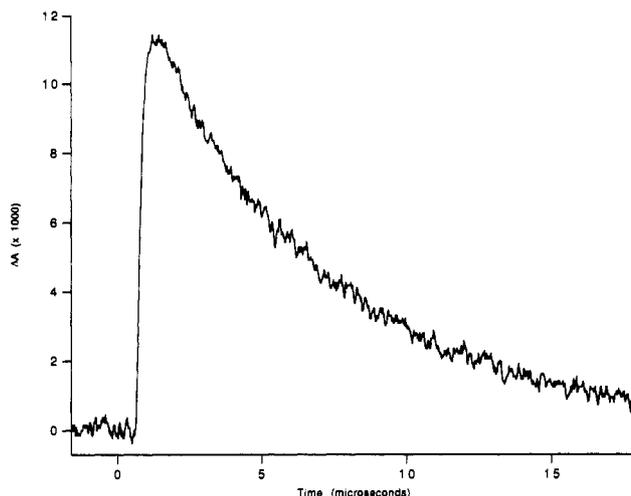


Figure 1. Transient decay for 7.9×10^{-4} M $\text{Rh}_2\text{b}_4^{2+}$ in CH_3CN , probing at 2173 cm^{-1} (average of 320 shots). Decay yields a best fit single-exponential lifetime of 6.1 μs .

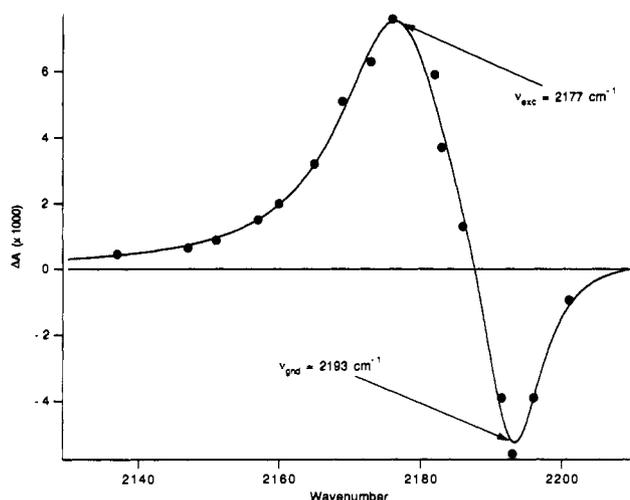


Figure 2. TRIR difference spectrum for 7.9×10^{-4} M $\text{Rh}_2\text{b}_4^{2+}$ in CH_3CN . The solid line is a calculated double-Lorentzian best fit to the data (●).

observation of multiphoton effects. We find, however, that the decrease in absorbance near the ground-state frequency displays a linear dependence on incident pulse energy. Identical behavior is observed for the increase in absorbance at 2177 cm^{-1} . Additionally, our observation of a 6- μs decay for the excited state indicates that we are observing behavior associated with the triplet state. Thus, under our experimental conditions, only the triplet state contributes to the observed TRIR spectrum.

There is one further complication that might arise: at sufficiently high concentrations, $\text{Rh}_2\text{b}_4^{2+}$ is known to form end-to-end dimers and higher oligomers.⁵ These effects, however, are not expected to be important for solutions of concentrations less than millimolar. Furthermore, the solutions used in this study (concentrations of 7.9×10^{-4} and 3.9×10^{-4} M) showed no evidence for oligomerization in their visible spectra. (Dimers of $\text{Rh}_2\text{b}_4^{2+}$ display a new absorbance band centered at 778 nm.⁵) No con-

[†] Isotope and Structural Chemistry Group.
^{*} Photochemistry and Photophysics Group.

- (1) Smith, D. C.; Gray, H. B. *Coord. Chem. Rev.* **1990**, *100*, 169.
- (2) Dalling, R. F.; Miskowski, V. M.; Gray, H. B.; Woodruff, W. H. *J. Am. Chem. Soc.* **1981**, *103*, 1595.
- (3) Dimer solutions were prepared and loaded into 1 mm path length infrared cells with CaF_2 windows in an inert-atmosphere glovebox to exclude oxygen from the samples.
- (4) Miskowski, V. M.; Nobinger, G. L.; Klinger, D. S.; Hammond, G. S.; Lewis, N. S.; Mann, K. R.; Gray, H. B. *J. Am. Chem. Soc.* **1978**, *100*, 485.
- (5) Lewis, N. S.; Mann, K. R.; Gordon, T. G., II; Gray, H. B. *J. Am. Chem. Soc.* **1976**, *98*, 7461.

Table I. Calculated Ground- and Excited-State Bond Lengths for $\text{Rh}_2\text{b}_4^{2+}$

vib	ν_{gnd} , cm^{-1}	ν_{exc} , cm^{-1}	r_{gnd} , Å	r_{exc} , Å	Δr , Å
$\nu(\text{Rh—Rh})$	79 ^a (0.189) ^b	144 ^a (0.629)	3.175	2.965	-0.210
$\nu(\text{Rh—C})$	467 ^a (1.381)	484 ^a (1.483)	2.253	2.231	-0.022
$\nu(\text{C}\equiv\text{N})$	2193 (18.31)	2177 (18.04)	1.132	1.134	+0.002

^a Values taken from ref. 2. ^b Values in parentheses are force constants in $\text{mdyn}/\text{Å}$.

centration-dependent differences in the TRIR results were observed.

The absorbance increase at 2177 cm^{-1} is assigned to the excited-state $\text{C}\equiv\text{N}$ stretch. The shift to lower energy in the excited-state vibration may be rationalized in terms of the excited-state electronic structure. The optically excited transition is the $^1A_{1g} \rightarrow ^1A_{2u}$ ($d\sigma^* \rightarrow p\sigma$) transition.⁶ The $^1A_{2u}$ state rapidly decays to the TRIR-observed $^3A_{2u}$ ($p\sigma$) state.⁴ The change from antibonding ($d\sigma^*$) to bonding ($p\sigma$) character along the Rh—Rh axis is consistent with the observed increase in the ground-state metal–metal frequency from 79 cm^{-1} to that in the excited-state of 144 cm^{-1} , indicating an increase in the Rh—Rh bond order.² The ($p\sigma$) metal–metal orbital that is populated in the excited state has the correct symmetry for overlap with the π systems of the $\text{C}\equiv\text{N}$ group of the isocyanide ligands. This overlap is, to a first approximation, lacking for the ($d\sigma^*$) metal–metal orbital, which is the HOMO of the ground state. Thus, increased backbonding from metal to isocyanide is expected in the excited state. This increased backbonding is manifested in the previously observed increase in the ground-state Rh—C stretching frequency from 467 cm^{-1} to the excited-state frequency of 484 cm^{-1} .² The additional electron density donated through π -backbonding is expected to be accommodated in an antibonding $2p\pi^*$ orbital of the $\text{C}\equiv\text{N}$ group, resulting in a somewhat reduced $\text{C}\equiv\text{N}$ force constant.⁷ It is therefore expected that, upon photoexcitation, the $\text{C}\equiv\text{N}$ stretching frequency will decrease. In fact, we observe a decrease from 2193 to 2177 cm^{-1} .

Knowledge of the excited-state $\text{C}\equiv\text{N}$ frequency completes the vibrational information required for determining the excited-state bond displacements occurring in $\text{Rh}_2\text{b}_4^{2+}$. From systems with known force constants for vibrations between two atoms with known bond distances, Woodruff and co-workers⁸ have developed a set of empirical rules that allows the calculation of unknown bond distances from measured force constants. The empirical results take the form of $r = A + B[\exp(-k/C)]$, where r is the bond distance in angstroms, k is the force constant in $\text{mdyn}/\text{Å}$, and A , B , and C are best fit coefficients determined for diatomic interactions between atoms of different rows.⁹ The results for the Rh—Rh, Rh—C, and $\text{C}\equiv\text{N}$ vibrations are summarized in Table I.

The calculations indicate that the largest displacements occur along the Rh—Rh bond (-0.210 Å) and between the Rh—C bond (-0.022 Å), while the $\text{C}\equiv\text{N}$ bond undergoes very little displacement ($+0.002\text{ Å}$). This is consistent with expectations in that little metal-to-ligand charge-transfer character is expected for this transition. However, no quantitative estimate of this displacement has been reported previously. Analysis of vibrational progressions resolved in low-temperature UV/vis spectra of the dimer suggested only an upper limit of 0.01 Å for the displacement of the $\text{C}\equiv\text{N}$ coordinate.⁶ A comparison of our results and the vibronic analysis underscores the importance of the ability to obtain excited-state vibrational spectra using TRIR spectroscopy in that much smaller displacement values may be estimated.

The accuracy of the displacement calculations and, thus, the picture of the excited-state geometry that they reveal are limited by the assumptions inherent in the application of the simple empirical rules. Application of these rules to our data implies that each vibration is solely a local stretching mode, rather than a normal-coordinate displacement involving several bond length and bond angle changes. It is, however, reasonable to expect that, upon shortening of the Rh—Rh bond in the excited state, the Rh—C≡N bond angle might change. Thus, some Rh—CN bending character could be mixed into the vibrational modes assumed to be of only local stretching character. Future work will be directed at extending the nanosecond TRIR studies to a series of Rh—Rh ligand-bridged systems in which the chain length of the diisocyanide bridge is varied to see how the steric constraints imposed by the bridge affect excited-state behavior in these systems.

Acknowledgment. We wish to thank Dr. David C. Smith for his donation of a sample of $\text{Rh}_2\text{b}_4^{2+}$ for these studies. This work was supported by Los Alamos National Laboratory under LDRD Grant X15D. K.C.G. gratefully acknowledges support by a LANL director's postdoctoral fellowship. This work was performed at LANL under the auspices of the U.S. Department of Energy.

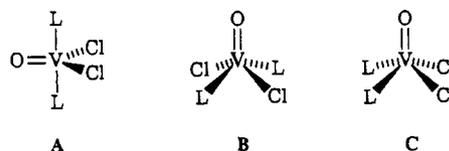
Contribution from the Department of Chemistry
and Ames Laboratory, Iowa State University,
Ames, Iowa 50011-3111

Unexpected Formation of a Novel Divanadium(IV) Monophosphine Complex

A. K. Fazlur-Rahman, V. G. Young, Jr., and J. G. Verkade*

Received September 5, 1991

While complexes of the type $\text{L}_n\text{V}(\text{O})\text{Cl}_2$, wherein L is a monodentate ($n = 1, 2$, or 3) or a bidentate neutral ligand, have been known for many years,¹ only a few such complexes containing phosphine ligands have been reported and no reports of stable arsine or stibine adducts exist. The only reported compounds containing phosphines include $(\text{dppe})(\text{H}_2\text{O})\text{V}(\text{O})\text{X}_2$ ($\text{X} = \text{Cl}, \text{Br}$),² $(\text{dppm})(\text{H}_2\text{O})\text{V}(\text{O})\text{Br}_2$,² $(\text{Ph}_3\text{P})_2\text{V}(\text{O})\text{Cl}_2$,³ $(\text{Ph}_2\text{MeP})_2\text{V}(\text{O})\text{Cl}_2$,³ and $(\text{dppm})\text{V}(\text{O})\text{Cl}_2$.³ $\text{L}_2\text{V}(\text{O})\text{Cl}_2$ complexes, wherein L is NMe_3 ⁴ and $\text{OC}(\text{NMe}_2)_2$,⁵ have been shown by X-ray diffraction means to display a trigonal bipyramidal (A) and a square pyramidal (B) geometry, respectively. However, no reports of X-ray structures



of the phosphine complexes were found. From IR data, the geometries of $(\text{Ph}_3\text{P})_2\text{V}(\text{O})\text{Cl}_2$ and $(\text{Ph}_2\text{MeP})_2\text{V}(\text{O})\text{Cl}_2$ have been

(6) Rice, S. F.; Miskowski, V. M.; Gray, H. B. *Inorg. Chem.* **1988**, *27*, 4704.
(7) Nakamoto, K. *Infrared and Raman Spectra of Inorganic and Coordination Compounds*, 4th ed.; Wiley: New York, 1986; p 272.
(8) Woodruff, W. H. Unpublished results. See also: Miskowski, V. M.; Dallinger, R. F.; Christoph, G. G.; Morris, D. E.; Spies, G. H.; Woodruff, W. H. *Inorg. Chem.* **1987**, *26*, 2127.
(9) A, B, and C are 1.077, 0.629, and 7.539, respectively, for two first-row elements (i.e. $\text{C}\equiv\text{N}$); 1.816, 1.461, and 2.610 for two interacting fourth-row elements (Rh—Rh); and 1.617, 1.040, and 2.812 for interactions between a first- and a fourth-row element (Rh—C).

(1) (a) Clark, R. J. H. In *Comprehensive Inorganic Chemistry*; Bailar, J. C., Emeleus, H. J., Nyholm, R. S., Eds.; Trotman-Dickinson, A. F.; Pergamon Press: Oxford, 1973; Vol. 3. (b) Boas, L. V.; Pessoa, J. C. In *Comprehensive Coordination Chemistry*; Wilkinson, G., Gillard, R. D., McCleverty, J. A., Eds.; Pergamon Press: Oxford, 1987; Vol. 3.
(2) Selbin, J.; Vigeo, G. *J. Inorg. Nucl. Chem.* **1968**, *30*, 1644.
(3) Cave, J.; Dixon, P. R.; Seddon, K. R. *Inorg. Chim. Acta* **1978**, *30*, L349.
(4) Drake, J. E.; Vekris, J.; Wood, J. S. *J. Chem. Soc. A* **1968**, 1000.
(5) Coetzer, J. *Acta Crystallogr.* **1970**, *B26*, 872.
(6) Kern, R. J. *J. Inorg. Nucl. Chem.* **1962**, *24*, 1105.